

## Supplementary Information

### **In Situ Grown CNTs and Electrodeposited MnO<sub>2</sub> on MXene-Carbon Nanofibers for Flexible Supercapacitors with High Energy Density**

Binhe Feng<sup>a</sup>, Deyang Zhang<sup>a,\*</sup>, Wenbo Guo<sup>a</sup>, Zhaorui Wang<sup>a</sup>, Jinbing Cheng<sup>b</sup>, HaiLong Yan<sup>b</sup>, Tao Peng<sup>a</sup>, Kangwen Qiu<sup>c</sup>, Feng Jing<sup>c</sup>, Yikai Ge<sup>a</sup>, Mengzhen Du<sup>a</sup>, Paul K. Chu<sup>d</sup>, Yongsong Luo<sup>a,b,\*</sup>

<sup>a</sup>Henan Joint International Research Laboratory of New Energy Storage Technology, Xinyang Normal University, Xinyang 464000, P. R. China. E-mail: zdy@xynu.edu.cn (D. Y. Zhang)

<sup>b</sup>Henan International Joint Laboratory of MXene Materials Microstructure, Collaborative Innovation Center of Intelligent Explosion-proof Equipment of Henan Province, Nanyang Normal University, Nanyang 473061, P. R. China. E-mail: ysluo@xynu.edu.cn (Y. S. Luo)

<sup>c</sup>College of Energy Engineering, Huanghuai University, Zhumadian, Henan 463000, China

<sup>d</sup>Department of Physics, Department of Materials Science & Engineering, and Department of Biomedical Engineering, City University of Hong Kong, Tat Chee Avenue, Kowloon, Hong Kong, China

### **Experimental Section**

## Materials

The  $\text{Ti}_3\text{AlC}_2$  powder (400 mesh) was purchased from Enwang New Materials Technology Co., Ltd. Manganese acetate tetrahydrate ( $\text{Mn}(\text{CH}_3\text{COO})_2 \cdot 4\text{H}_2\text{O}$ , 99%), anhydrous sodium sulfate ( $\text{Na}_2\text{SO}_4$ ,  $\geq 99.0\%$ ), N, N-dimethyl formamide (DMF, 99.9%), Cobaltous nitrate hexahydrate ( $\text{Co}(\text{NO}_3)_2 \cdot 6\text{H}_2\text{O}$ , 99%), 2-Methylimidazole ( $\text{C}_4\text{H}_6\text{N}_2$ , 98%) and polyacrylonitrile (PAN,  $M_w = 150,000$ ) were provided by Aladdin.

All the reagents were analytical grade and used without further purification.

## Synthesis of $\text{Ti}_3\text{C}_2\text{T}_x$ MXene

The  $\text{Ti}_3\text{C}_2\text{T}_x$  nanosheets were produced by LiF/HCl etching and exfoliating  $\text{Ti}_3\text{AlC}_2$ . In brief, LiF (1 g) was added to 30 ml of 9 mol/L hydrochloric acid and heated to 36 °C under stirring. 40% HF (5 mL) was then added when the solution became clear. After 1 g of  $\text{Ti}_3\text{AlC}_2$  MAX was added, the reaction proceeded for 12 h. The black solution was washed repeatedly with deionized water and centrifuged at 5,000 rpm until the  $\text{pH} \geq 6$ . The dark green mud deposit was collected and transferred to a bottle under Ar and sonicated under Ar for an hour. It was washed repeatedly with deionized water and centrifuged at 10,000 rpm to collect the product. To obtain the solution for electrospinning, the product obtained from the previous step was washed three times with DMF, and the concentration was adjusted to  $20 \text{ mg mL}^{-1}$ .

## Synthesis of CNTs-PC/MX /CF

The CNTs-PC/MX/CF samples were synthesized by growing Co-MOF on a  $\text{Ti}_3\text{C}_2\text{T}_x/\text{CNFs}$  thermally stable spinning mat and then one-step carbonization and catalysis. In brief, polyacrylonitrile (0.6 g) was dispersed in 5 mL of the  $\text{Ti}_3\text{C}_2\text{T}_x$  solution, stirred continuously for 6 h, and placed in a 5 mL plastic syringe with an 18 G blunt-tip needle. A positive voltage (20 kV) was applied to the needle tip, and the copper collector roller covered by an aluminum foil was grounded. The distance between the needle tip and collector was 12.5 cm, and the infusion rate of the solution was  $0.8 \text{ mL h}^{-1}$ . The samples were electrospun at a relative humidity below 30%. The electrospun mats were stabilized in air at  $267^\circ\text{C}$  for 2 h at a ramping rate of  $3^\circ\text{C min}^{-1}$ .

Two beakers were filled with 40 mL of deionized water. 2-methylimidazole (1.313 g) was added to one beaker, while 0.249 g of  $\text{Co}(\text{NO}_3)_2 \cdot 6\text{H}_2\text{O}$  (0.249 g) was placed in the second beaker. The two solutions were mixed quickly and stirred for 1 minute. A piece of stabilized electrospun mat was placed vertically in the solution and left for 5 hours. A crucible containing 0.35 g of melamine was placed upstream, and another containing a sample was placed downstream. It was heated to  $750^\circ\text{C}$  for 90 minutes at a heating rate of  $2^\circ\text{C min}^{-1}$ .

### **Synthesis of $\text{MnO}_2@\text{CNTs-PC/MX/CF}$**

The  $\text{MnO}_2$  nanoflowers were prepared onto the surface of CNTs-PC/MX/CF by anodic electrodeposition (constant current) using a CHI660E electrochemical workstation in a solution (60 mL) containing manganese acetate (0.001 M) and sodium

sulfate (0.001 M) at 1.2 V(SHE) for 1200 s at room temperature. The size of the electrodeposited composite electrode substrate was 1.5 x 1 cm<sup>2</sup>.

### **Fabrication of all-solid-state asymmetric supercapacitors**

The all-solid-state button asymmetric supercapacitors (ASCs) were assembled with MnO<sub>2</sub>@CNTs-PC/MX/CF as the positive and CNTs-PC/MX/CF as the negative electrodes, respectively, and 1 M Na<sub>2</sub>SO<sub>4</sub> as the electrolyte. The flexible all-solid-state Na<sub>2</sub>SO<sub>4</sub>/PVA contained a gel electrode. The Na<sub>2</sub>SO<sub>4</sub>/PVA gel electrolyte was fabricated by the following steps. The polyvinyl alcohol (PVA) powder (2 g) was dissolved in 20 mL of DI water and heated to 90 °C under stirring until the solution became clear. Subsequently, aqueous Na<sub>2</sub>SO<sub>4</sub> (10 mL, 0.1 g mL<sup>-1</sup>) was added dropwise under constant stirring, and the Na<sub>2</sub>SO<sub>4</sub>/PVA gel solution was applied between the electrodes (MnO<sub>2</sub>@Ti<sub>3</sub>C<sub>2</sub>T<sub>x</sub>/CNFs and AC@NC). After drying at room temperature for 1 h to solidify the gel, a firm all-solid-state ASC was obtained.

### **Materials characterization**

The crystalline structure and phase of the composites were identified by X-ray diffraction (XRD, Bruker D2 PHASER) using Cu-K<sub>α</sub> ( $\lambda = 1.5418 \text{ \AA}$ ) radiation at 40 kV, 40 mA, and  $2\theta$  between 5° and 80° at room temperature. Raman scattering was carried out on the INVIA Raman microprobe (Renishaw Instruments) with a 532 nm laser source and a 50× objective lens at a laser power of 5%. The chemical composition was determined by X-ray photoelectron spectroscopy (XPS, K-ALPHA

0.5 eV) with a resolution of 0.3-0.5 eV using a monochromatic aluminum X-ray source.

The morphology was examined by field-emission scanning electron microscopy (SEM, Hitachi S-4800) and transmission electron microscopy (TEM, FEI Tecnai G2 F20), and elemental analysis was carried out by energy-dispersive X-ray spectroscopy (EDS, Bruker QUANTAX) on the TEM.

### Electrochemical assessment

The electrochemical properties of  $\text{MnO}_2@\text{MX}/\text{CF}$ ,  $\text{MnO}_2@\text{PC-MX}/\text{CF}$ , and  $\text{MnO}_2@\text{CNTs}/\text{PC-MX}/\text{CF}$  were determined in 1 M  $\text{Na}_2\text{SO}_4$  using the traditional three-electrode system at 25 °C. The platinum and saturated calomel electrodes were the counter and reference electrodes, respectively, in the CHI660E electrochemical workstation. The asymmetric supercapacitor was assembled with  $\text{MnO}_2@\text{CNTs-PC}/\text{MX}/\text{CF}$  as the positive electrode,  $\text{CNTs-PC}/\text{MX}/\text{CF}$  as the negative electrode, and  $\text{PVA}/\text{Na}_2\text{SO}_4$  gel electrolyte as the electrolyte.

Cyclic voltammetry (CV) was performed in the voltage ranges between -1 and 0 as well as 0 and 1 V. The GCD curves were acquired according to the CV window. Electrochemical impedance spectroscopy (EIS) was conducted at frequencies between 0.01 Hz and 100 kHz. The specific capacitance ( $C_m$ ,  $\text{F g}^{-1}$ ) was calculated by the following equation:

$$C_m = \frac{I \times \Delta t}{m \times \Delta V} \quad (1)$$

where  $I$  (A) is the applied current,  $\Delta t$  (s) is the discharging time,  $\Delta V$  (V) is the discharging potential range, and  $m$  (g) is the total mass of active materials. The

theoretical pseudo-capacitance was calculated as follows:

$$C = \frac{n \times F}{M \times V} \quad (2)$$

where  $n$  (mol) is the number of electrons transferred in the redox reaction,  $M$  ( $\text{g mol}^{-1}$ ) is the molar mass of the materials,  $F$  ( $\text{C. mol}^{-1}$ ) is Faraday's constant, and  $V$  (V) is the operating voltage window, respectively. The charge balance between the two electrodes should follow the relationship  $q^+ = q^-$ , where  $q$  is the charge stored in the electrode calculated by the following equation:

$$q = C_m \times \Delta E \times m \quad (3)$$

where  $C_m$  ( $\text{F g}^{-1}$ ) is the specific capacitance,  $\Delta E$  (V) is the potential range in the charging/discharging process, and  $m$  (g) is the mass loading of the active materials. The ideal mass ratio of the active materials on the positive ( $\text{MnO}_2@\text{Ti}_3\text{C}_2\text{T}_x/\text{CNFs}$ ) and the negative electrode (AC) in the asymmetric supercapacitor ( $m^+/m^-$ ) was calculated by the equation:

$$\frac{m^+}{m^-} = \frac{\Delta E_- \times C_-}{\Delta E_+ \times C_+} \quad (4)$$

The energy density ( $E$ ) and power density ( $P$ ) were calculated by the following equations:

$$E = \frac{1}{2 \times 3.6} C_m (\Delta E)^2 \quad \text{and} \quad (5)$$

$$P = \frac{E \times 3600}{\Delta t}$$

where  $E$  ( $\text{Wh kg}^{-1}$ ) is the energy density,  $C_m$  ( $\text{F g}^{-1}$ ) is the specific capacitance,  $\Delta V$  (V) is the operating potential window,  $P$  ( $\text{kW kg}^{-1}$ ) is the power density, and  $\Delta t$  (s) is the discharging time.

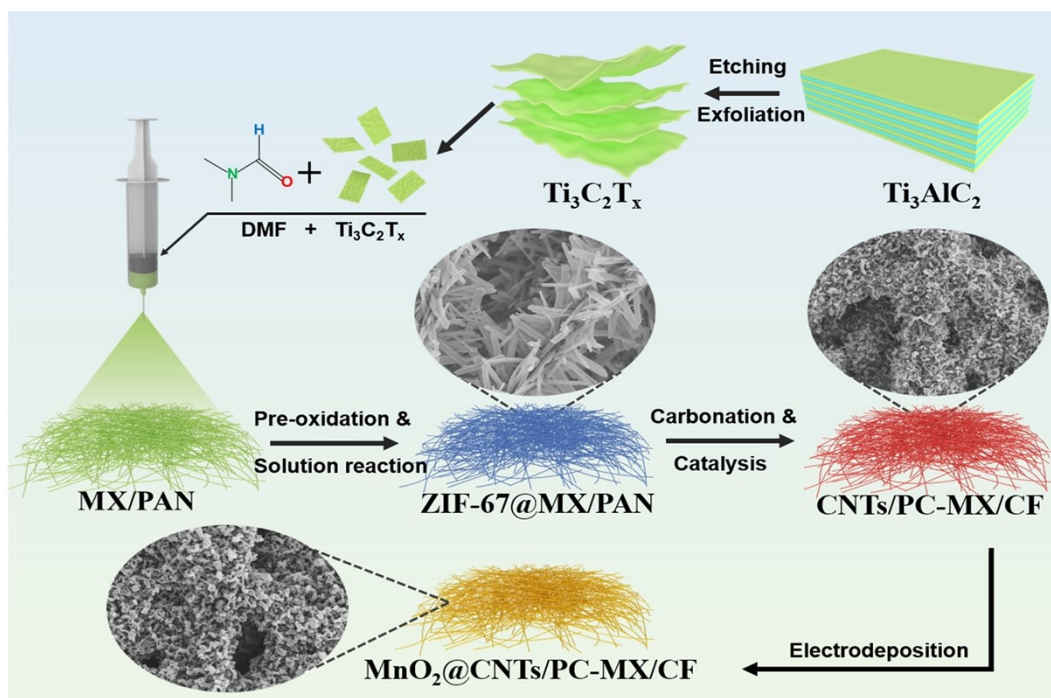


Fig S1. Schematic illustration of the processing of  $\text{MnO}_2@\text{CNT/PC-MX/CF}$

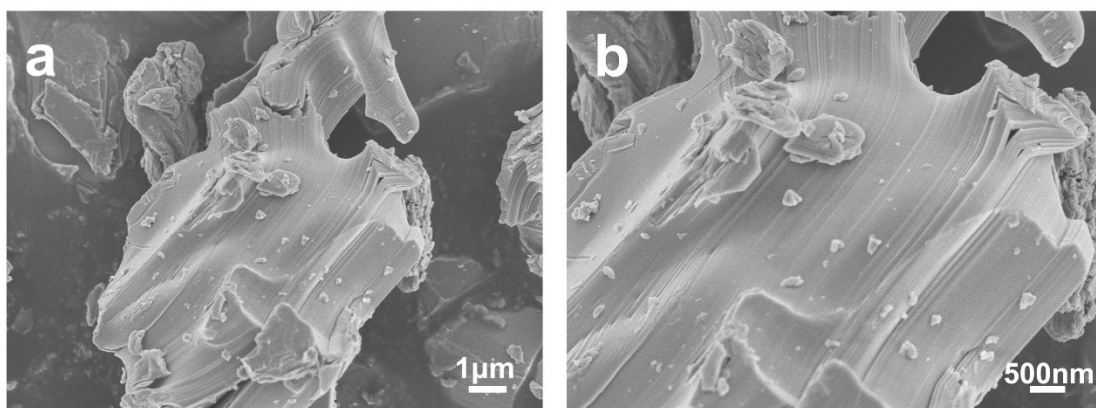


Figure S2. (a-b) SEM images of  $\text{Ti}_3\text{AlC}_2$ .

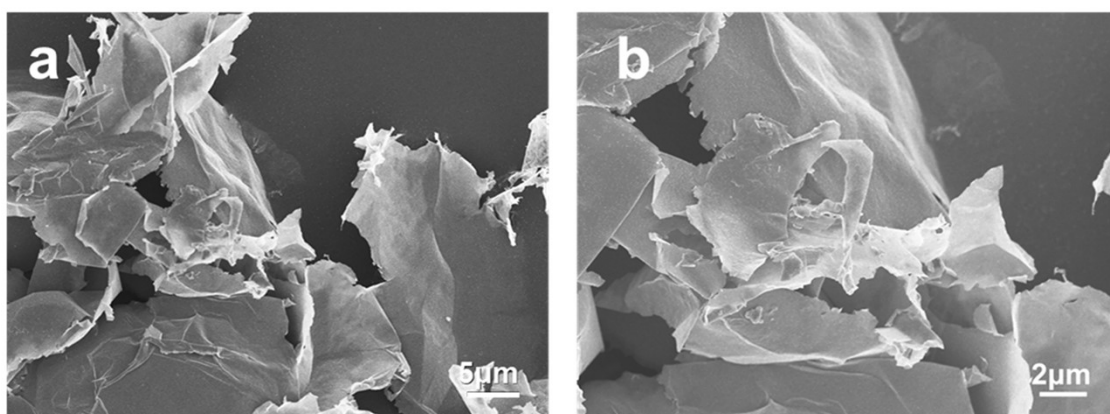


Figure S3. (a-b) SEM images of  $\text{Ti}_3\text{C}_2\text{T}_x$  MXene.



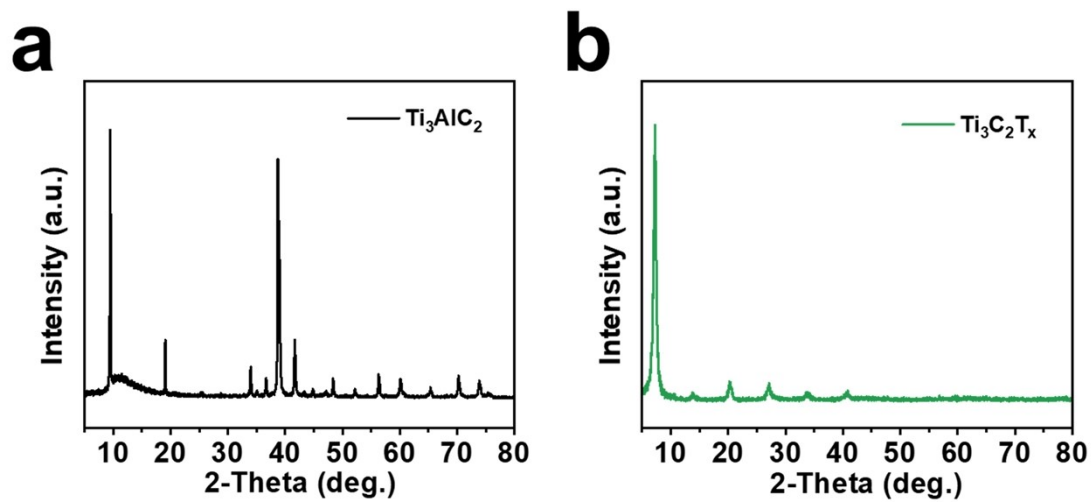


Figure S4. (a-b) XRD images of  $\text{Ti}_3\text{AlC}_2$  and  $\text{Ti}_3\text{C}_2\text{T}_x$  MXene

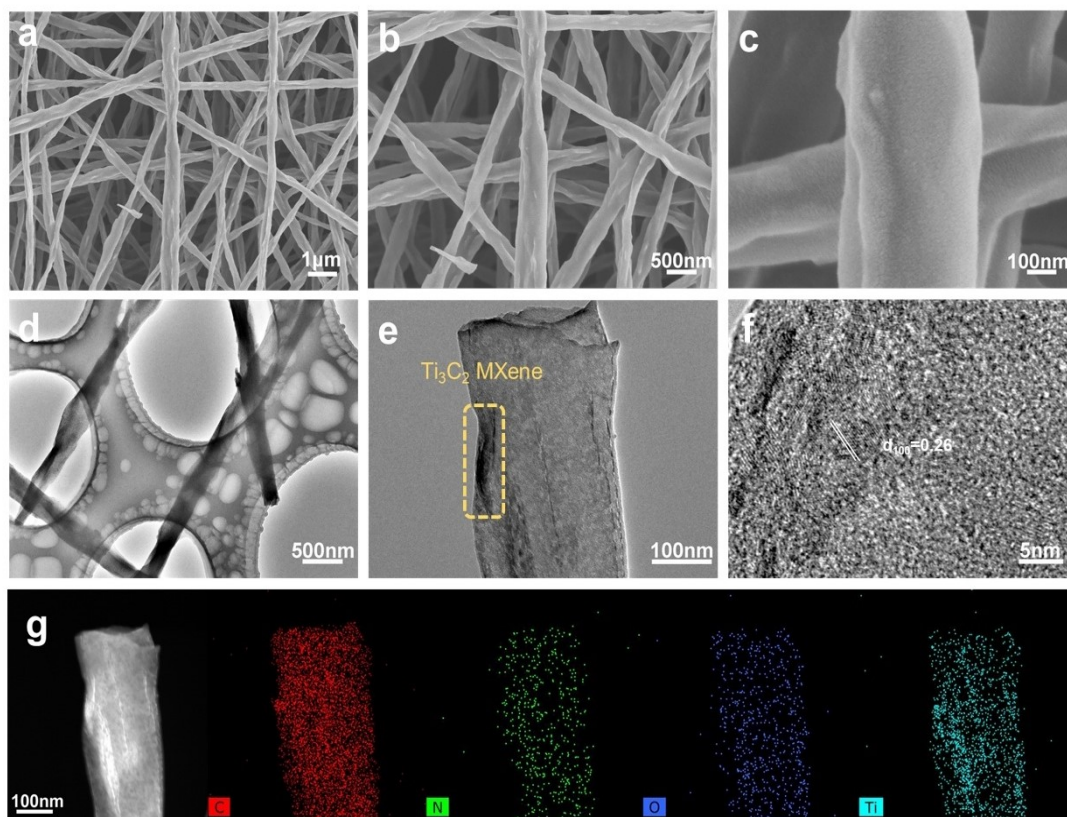


Figure S5. (a-c) SEM images of MX/CF; (d-f) TEM images of MX/CF; (g) EDS elemental maps of MX/CF.

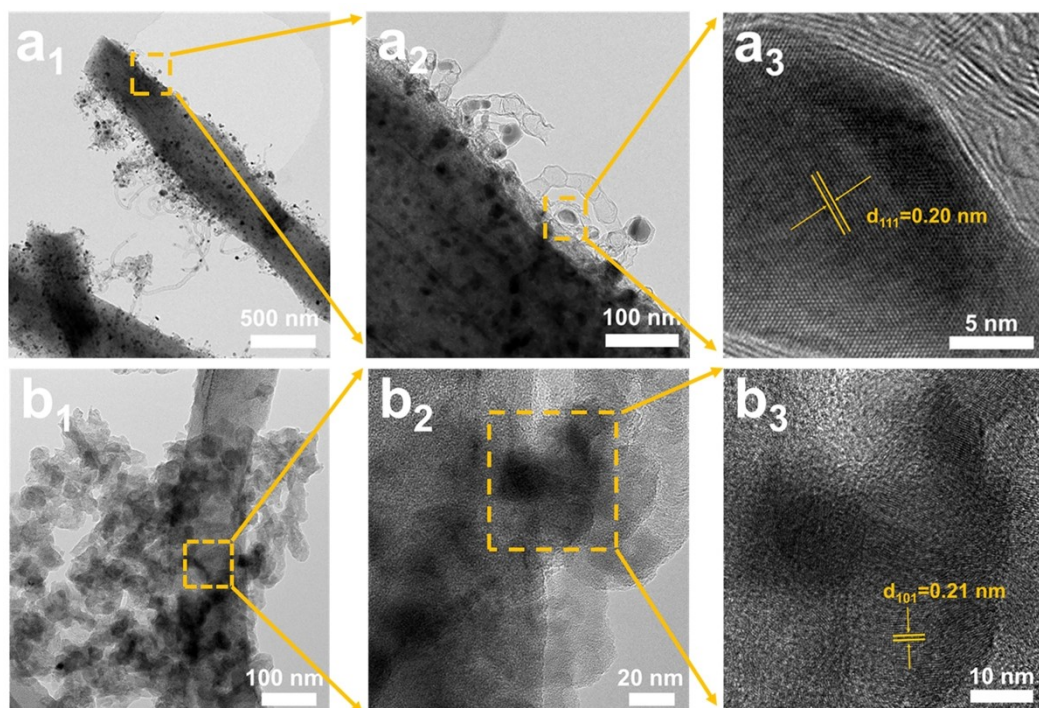


Fig S6. (a1-a2) TEM images of CNTs/PC-MX/CF; (b1-b2) TEM images of  $\text{MnO}_2$ @CNTs/PC-MX/CF

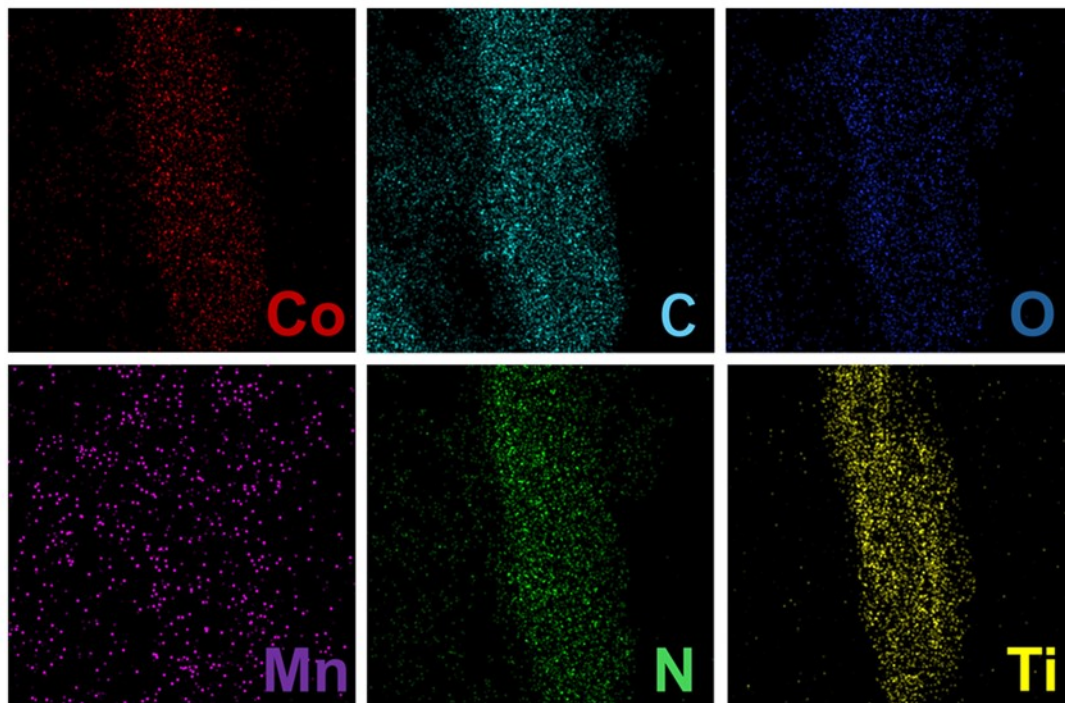


Figure S7. EDS elemental maps of  $\text{MnO}_2$ @CNTs/PC-MX/CF.

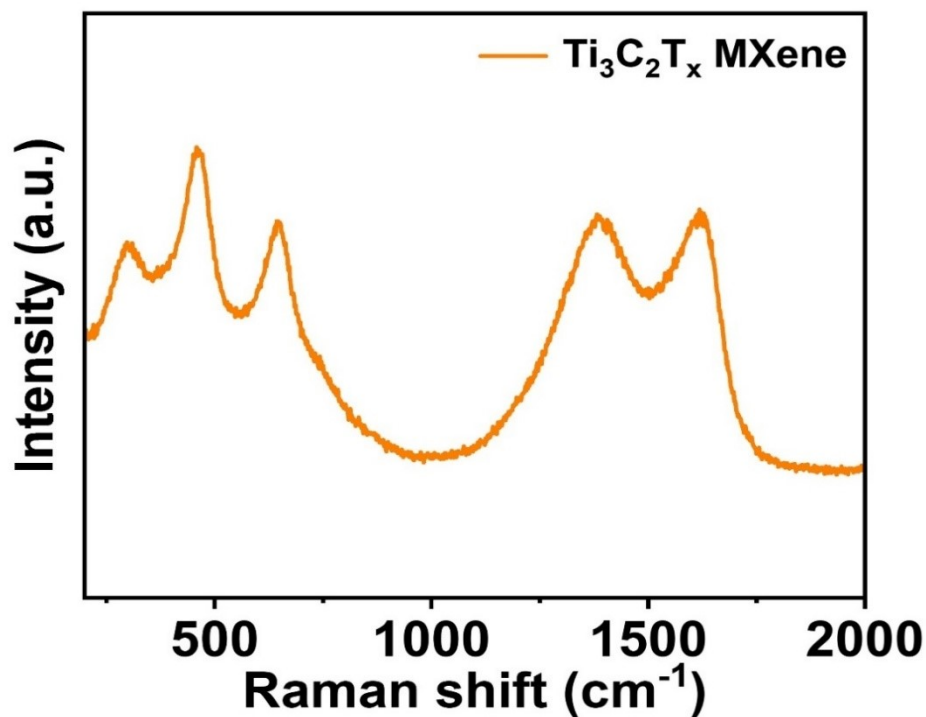


Figure S8. Raman scattering spectra of  $\text{Ti}_3\text{C}_2\text{T}_x$  MXene.

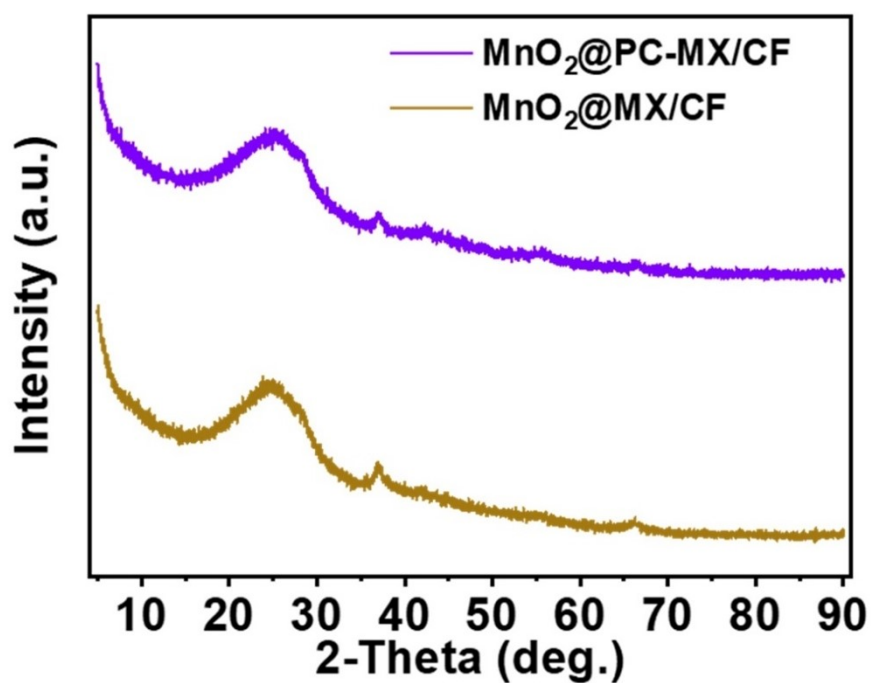


Figure S9. XRD patterns of the control samples:  $\text{MnO}_2@\text{PC-MX/CF}$  (derived from carbonized  $\text{ZIF-67}@\text{MX/PAN}$  without CNT growth) and  $\text{MnO}_2@\text{MX/CF}$  (electrodeposited directly on the MX/CF substrate).

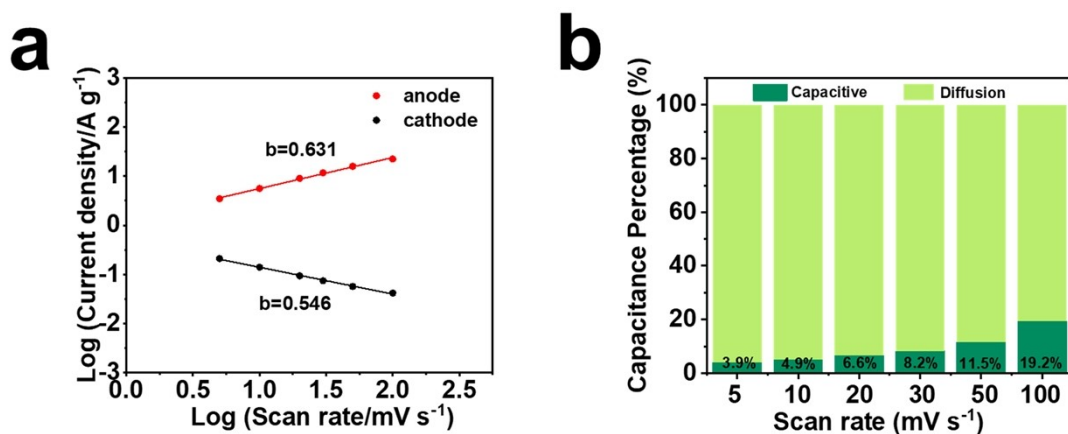


Figure S10. (a)  $b$  value; (b) Percentages of diffusion-controlled and capacitance-controlled processes at various sweeping rates.

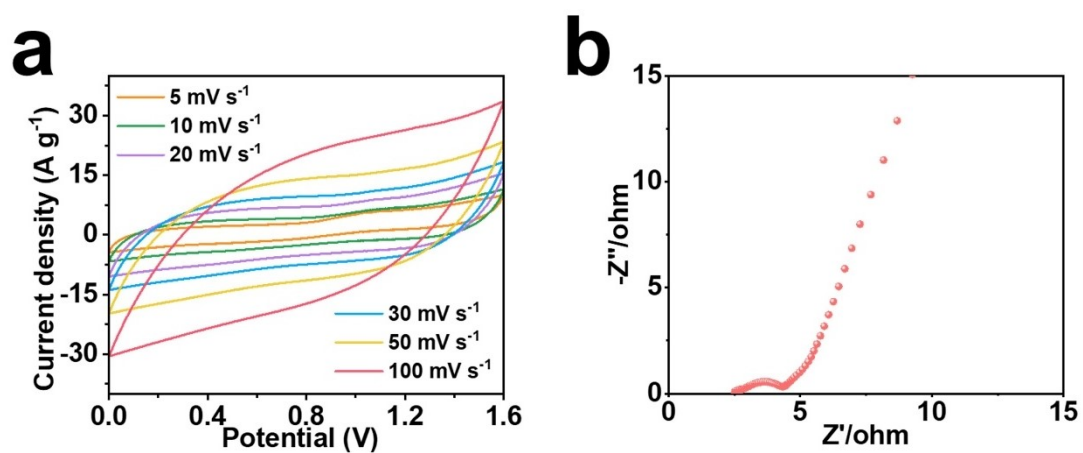


Figure S11. (a) CV curves of ASC at different current densities and (b) Nyquist plot of ASC.



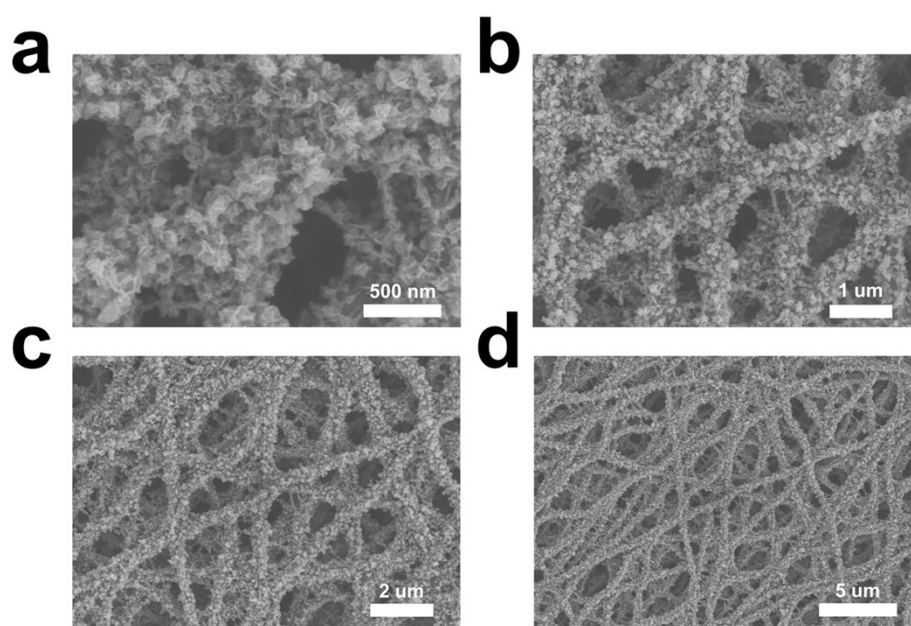


Figure S12. SEM image of the material after cycling.

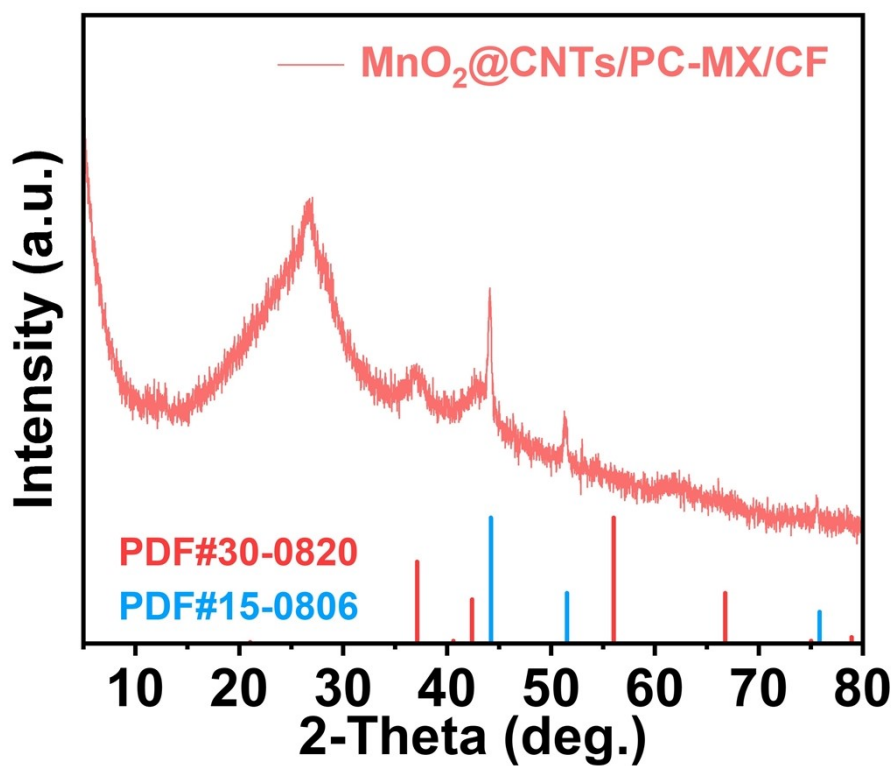


Figure S13. XRD pattern of the material after cycling